

Analysis of shot-noise suppression in disordered quantum wires

L. Bonci^a, G. Fiori^a, M. Macucci^{a,*}, G. Iannaccone^a, S. Roddaro^b, P. Pingue^b,
V. Piazza^b, M. Cecchini^b, F. Beltram^b

^a*Dipartimento di Ingegneria dell'Informazione, Università degli Studi di Pisa, Via Diotisalvi, 2, I-56122 Pisa, Italy*

^b*NEST-INFN, Scuola Normale Superiore, I-56126 Pisa, Italy*

Abstract

We present a numerical model for shot-noise suppression in a semiconductor quantum wire, based on parameters obtained from a purposely fabricated and characterized device. Shot-noise suppression is studied as a function of the voltage applied to the depletion gates forming the wire in a GaAs/AlGaAs heterostructure, of the dopant concentration in the δ -doping layer, and of the length of the wire. Results provide an understanding of why a conclusive experimental demonstration of diffusive transport with $\frac{1}{3}$ suppression of shot noise in mesoscopic semiconductor devices has so far proved to be elusive.

© 2003 Published by Elsevier B.V.

PACS: 72.70.+m; 73.23.-b; 72.20.-i; 73.63.Nm

Keywords: Shot noise; Diffusive transport; Quantum wire; Noise suppression

Recent theoretical activities have focused on the investigation of shot-noise suppression in several types of nanoscale devices. In particular, the suppression factor for conduction in the diffusive regime has been extensively studied applying Random Matrix Theory or by means of large-scale numerical calculations on structures containing randomly placed hard-wall scatterers.

However, no detailed simulation of noise has so far been performed on realistic structures, in which carrier scattering is due to irregularities in the potential that are the consequence of randomly distributed donors, although a very refined analysis of the conductance of such structures can be found in the literature [1,2]. A single experimental paper [3] can be found in the

literature on the measurement of shot-noise suppression in a semiconductor diffusive quantum wire: Liefrink et al. observed, as a function of gate voltage, a suppression varying between 0.2 and 0.4 times the full shot-noise value. Such a result, although interesting, did not therefore represent conclusive evidence for the observation of diffusive transport in a semiconductor nanostructure, also because the estimated inelastic scattering length was less than the length of the wire.

We have developed a model for the investigation of conductance and noise in a quantum wire with elastic scattering due to donors located in a δ -doping layer. This model has been derived from the description of an actual device, which has been fabricated and experimentally characterized, from the point of view of the dependence of conductance on gate voltage, but not yet from that of the noise behavior.

* Corresponding author. Tel.: +39-50-568537; fax: +39-50-568522.

E-mail address: macucci@mercurio.iet.unipi.it (M. Macucci).

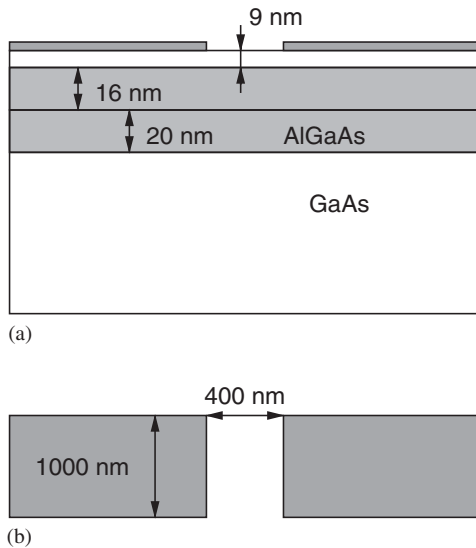


Fig. 1. (a) Heterostructure layers and (b) gate layout.

We have compared the experimentally measured conductance with the results of the numerical simulation, in order to calibrate the values of the surface charge density and of the donor concentration in our model, and to validate the overall simulation approach. Once reasonable agreement has been obtained between experimental conductance and the numerical result, we have used our code to investigate the shot-noise suppression in the device.

The quantum wire has been fabricated by evaporation of a metallic (Al) split gate on a modulation-doped heterostructure containing a two-dimensional electron gas (2DEG) confined at a $\text{Al}_{0.3}\text{Ga}_{0.7}\text{As}/\text{GaAs}$ heterojunction 45 nm below the wafer surface. Conduction-band electrons have been provided by a Si delta-doping layer embedded 20 nm above the heterojunction. The layer structure is reported in Fig. 1(a) and the gate layout is shown in Fig. 1(b). The Hall carrier density and mobility measured at 1.7 K after illumination are $5.8 \times 10^{11} \text{ cm}^{-2}$ and $9 \times 10^5 \text{ cm}^2/\text{V s}$, respectively. The conductance of the device has been measured at 1.5 K with a standard two-wire lock-in technique at an excitation level of 30 μV at 17.2 Hz, as a function of the voltage applied to the split gate.

Since the length of the wire is about 1 μm , which we assume to be shorter than the inelastic scattering

length in the 2DEG, electrons undergo only elastic scattering due to irregularities in the potential created by the donors.

Inclusion of the detailed effect of the donors into the Poisson solver used to compute the electrostatic potential in the structure would require too fine a mesh, therefore we have resorted to an approximate approach, in which the Poisson equation is solved considering a uniform average donor density, and then the contribution of the discrete donors is included by means of a semi-analytical approach that takes into account screening from the 2DEG, and from the effect of partial ionization of the donor layer itself.

The Poisson equation has been solved in the three-dimensional domain: since quantum confinement is strong along the direction perpendicular to the AlGaAs/GaAs interface, the density of states is a sum of well-separated 2D subbands. In the region where the 2DEG forms, we have thus solved the Schrödinger equation in the vertical direction, within the framework of density functional theory, in order to compute the sub-band profiles. In the rest of the domain the total charge concentration has been computed semiclassically. We have then obtained the self-consistent solution of the Poisson–Schrödinger equation using the Newton–Raphson method with a predictor/corrector algorithm close to that proposed in Ref. [4] and described in a previous paper [5].

Devices with a 2DEG in close proximity of the surface are strongly influenced by the presence of surface states. We have included the effect of the surface states, implementing a model typically applied to metal–semiconductor interfaces [6] and based on two parameters: an effective work function Φ^* (assumed to be 4.85 eV in the following) and a uniform density of surface states per unit area per unit energy D_s . The effective work function represents the difference between the Fermi level E_F at the surface and the vacuum energy E_0 when the surface charge density is zero. We have made the additional assumption that the surface states below Φ^* behave as donors and all surface states above Φ^* behave as acceptors. Assuming that the electric field vanishes outside the device, we can limit our simulation domain to the semiconductor region and apply the following Neumann boundary condition at the air–semiconductor interface:

$$\frac{\partial \phi}{\partial x} = e \frac{D_s}{\epsilon} [\Phi^* + E_F - E_0], \quad (1)$$

where ϕ is the electrostatic potential, e is the electron charge, and ε is the material permittivity. From the Poisson solver we obtain that only about 50% of the donors is actually ionized. Partial ionization leads to further screening of the action of the ionized impurities, as will be discussed in the following.

Let us now introduce the procedure we have followed for the inclusion of the effect of donor discreteness in a more detailed way. Our approach consists in adding to the smooth potential obtained from the Poisson solver the effect of a random distribution of charges adjusted in such a way as to keep the mean value of the potential unchanged. This result has been accomplished generating a random distribution of elementary charges located in the δ -doped layer with a concentration corresponding to that of the actually ionized donors, and computing their contribution to the potential as the superposition of the effects of each single charge. We have then subtracted from this contribution its mean value (computed from a spatial average), thus obtaining a fluctuating potential with zero average. This is finally added to the smooth solution obtained from the Poisson solver.

While evaluating the contribution to the potential from the impurities, we have taken into consideration screening from the 2DEG following Ref. [11], in which analytical expressions for the potential perturbation produced in a 2DEG by an external point charge are provided. In the hypothesis of a degenerate 2D electron system at very low temperature, the proper expression for the screened potential in the 2DEG plane is

$$\Phi(r) = \frac{Ze}{4\pi\varepsilon} \int_0^\infty dx (x+s)^{-1} J_0(xr) \exp(-xd), \quad (2)$$

where we have chosen a polar coordinate system in which r is the distance from the orthogonal projection of the donor position onto the 2DEG plane; Z indicates the donor charge, J_0 is the Bessel function of order 0, d the distance between the 2DEG and the donor layer, and s the screening length. This last parameter in the quantum limit at zero temperature does not depend on carrier concentration and can be written as $s = 2n_v m^* e^2 / (\hbar^2 \varepsilon)$, where n_v is the sub-band degeneracy and m^* the effective mass. We have to consider that, as we have already mentioned, there is further screening, due to the partial ionization of the donor layer. It is very difficult to directly evaluate such a contribution,

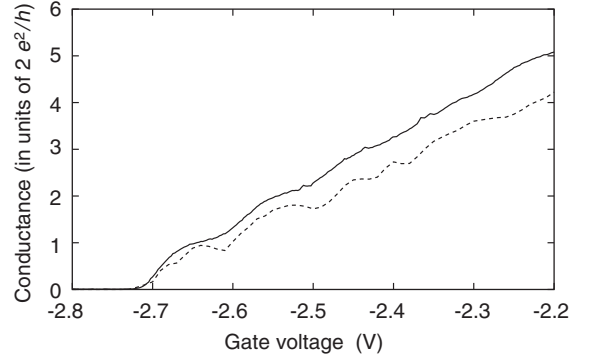


Fig. 2. Comparison between the experimental (solid curve) and simulated (dashed curve) conductance of the quantum wire as a function of gate voltage.

and we have resorted to a fitting parameter, finding the best match with the suppression of conductance steps. In this way, we have obtained a further reduction of the potential due to the ionized impurities by a factor 0.67.

The transmission matrix t for the thus obtained potential landscape has been evaluated with a recursive Green's function technique [7] and the conductance has then been computed on the basis of the Landauer–Büttiker formula:

$$G = 2 \frac{e^2}{h} \sum_{ij} |t_{ij}|^2, \quad (3)$$

where h is Planck's constant. In Fig. 2 the experimental (a) and simulated (b) conductance of the wire are reported as a function of the gate voltage: the effects of a finite temperature $T = 1.5$ K have been included by means of averaging over the derivative of the Fermi function within an interval of width $10 k_B T$ (k_B being the Boltzmann constant), centered around the Fermi energy.

The doping concentration N_s in the δ -doping layer and the density of surface states per unit area per unit energy D_s have been tuned in order to obtain a reasonable match between theoretical and experimental results, with $N_s = 1.13 \times 10^{12} \text{ cm}^{-2}$, and $D_s = 0.5 \times 10^{14} \text{ m}^{-2} \text{ eV}^{-1}$. We notice that conductance quantization is partially washed out due to discrete doping and finite temperature: this effect is very similar in the theoretical and in the experimental conductance curves, thus supporting the validity of our model.

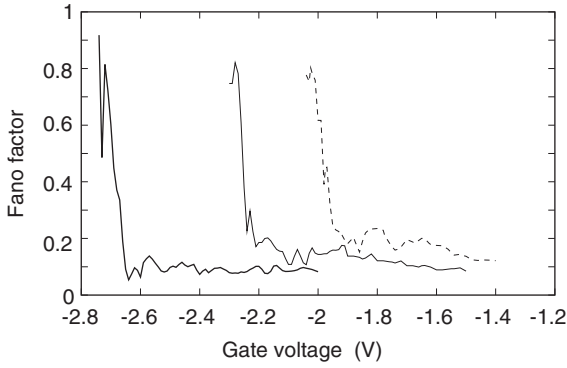


Fig. 3. Fano factor as a function of gate voltage for dopant density $N_s = 1.13 \times 10^{12} \text{ cm}^{-2}$ (thick solid curve), $N_s = 1.08 \times 10^{12} \text{ cm}^{-2}$ (thin solid curve), and $N_s = 1.05 \times 10^{12} \text{ cm}^{-2}$ (dashed curve).

The low-frequency shot-noise current power spectral density S_I has been computed as

$$S_I = 4 \frac{e^2}{h} |eV| \sum_i T_i (1 - T_i), \quad (4)$$

where V is the applied voltage and the T_i coefficients are obtained by diagonalizing the $t^\dagger t$ matrix [8]. According to Schottky's theorem, the full shot-noise $S_{I_{fs}}$ is given by $S_{I_{fs}} = 2qI$, where the current I can be obtained as $I = GV$. In this diagonal representation the conductance given by Eq. (3) can be written as

$$G = 2 \frac{e^2}{h} \sum_i T_i \quad (5)$$

and therefore the ratio γ of the actual noise power spectral density to the full shot-noise power spectral density, usually defined ‘‘Fano factor’’, reads

$$\gamma = \frac{\langle \sum_i T_i (1 - T_i) \rangle}{\langle \sum_i T_i \rangle}. \quad (6)$$

We point out that, if we want to compare to experimental results, correct averaging is over energies, weighted with the derivative of the Fermi function, rather than over an ensemble of devices, as usually done in the literature [9,10] for comparison with analytical results. Indeed, measurements are performed on a single device, with separate thermal averaging for the power spectral density and for the current.

In Fig. 3 the Fano factor is reported, as a function of the gate voltage, for the same parameters as

those used for fitting the conductance results (thick solid curve), and also for two reduced values of doping: $N_s = 1.08 \times 10^{12} \text{ cm}^{-2}$ (thin solid curve) and $N_s = 1.05 \times 10^{12} \text{ cm}^{-2}$ (dashed curve). Decreasing the doping concentration leads to an increase of the pinch-off voltage, as it would be expected, and to relatively minor variations in the noise behavior. Near the pinch-off voltage the Fano factor is maximum, approaching unity, since transport is mainly due to tunneling through the top of the saddle potential defining the bottom of the wire. As the transport reaches a condition intermediate between ballistic and diffusive, with increasing gate voltage, the Fano factor decreases, approaching an asymptotic value lower than the $\frac{1}{3}$ value expected for the purely diffusive case. This can be attributed to the relatively small amplitude of the perturbations produced in the confinement potential by the donors, which are therefore unable to cause strong enough scattering [12].

In order to investigate whether the diffusive regime can be reached in longer wires, we have repeated the noise calculations for ‘‘stretched’’ potential landscapes obtained by extending the length of the central region. In other words, we have inserted an additional section of length L in the middle of the wire, with the same transverse confinement potential as that originally present in this region and with a random distribution of dopants characterized by the same concentration as for the rest of the wire. We assume that the total length of the resulting wire is still less than the inelastic scattering length. Results for the Fano factor as a function of gate voltage (for $N_s = 1.08 \times 10^{12} \text{ cm}^{-2}$) are shown in Fig. 4, for $L = 0$ (a), $L = 2 \mu\text{m}$ (b), and $L = 4 \mu\text{m}$ (c). We notice that the increased length leads to an increase in the Fano factor, but the asymptotic value still lies well below the $\frac{1}{3}$ diffusive limit (dotted line). In a small interval of gate voltage values, around (-2 V) , the longer wires seem to exhibit a Fano factor around $\frac{1}{3}$, but there is no well-defined plateau.

Noise measurements on the available wire have not been performed yet, due to the very challenging requirements in terms of temperature, in order to reduce thermal noise below shot noise, and in terms of equipment sensitivity. We are currently working on the definition of the instrumentation requirements needed to achieve a precision sufficient for the validation of our theoretical results.

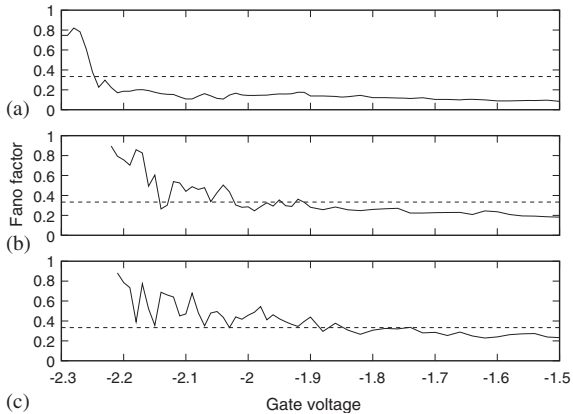


Fig. 4. Fano factor as a function of gate voltage for the original wire (a), for a wire stretched in length by $2 \mu\text{m}$ (b) and for a wire stretched by $4 \mu\text{m}$ (c); the dotted line indicates the diffusive limit of $\frac{1}{3}$.

We have developed a numerical model for transport and noise in a quantum wire, including the effect of randomly distributed donors. Adjustable model parameters, in particular donor concentration in the δ -doping layer and surface state density, have been tuned to match the experimental results for conductance obtained on a purposely fabricated and characterized quantum wire. From our calculations, the Fano factor for shot-noise suppression appears to vary, as a function of the voltage applied to the depletion gates, from values close to unity down to below 0.1, but in none of the cases taken into consideration the asymptotic diffusive limit of $\frac{1}{3}$ is reached over an extended interval of gate voltages, although for longer wires

we seem to get closer to it. If the length of the wire is further increased, however, there is a risk of going beyond the inelastic scattering length and therefore switching to a dissipative transport regime. Work is in progress to establish the feasibility of noise measurement on the available sample and on other quantum wires, with the aim of providing validation of our numerical model.

References

- [1] J.H. Davies, J.A. Nixon, *Phys. Rev. B* 39 (1989) 3423.
- [2] M.J. Laughton, J.R. Barker, J.A. Nixon, J.H. Davies, 44, (1991) 1150.
- [3] F. Liefvink, J.I. Dijkhuis, M.J.M. de Jong, L.W. Molenkamp, H. van Houten, *Phys. Rev. B* 49 (1994) 14066.
- [4] A. Trellakis, A.T. Galick, A. Pacelli, U. Ravaioli, *J. Appl. Phys.* 81 (1997) 7800.
- [5] G. Fiori, G. Iannaccone, M. Macucci, S. Reitzenstein, S. Kaiser, M. Kesselring, L. Worschech, A. Forchel, *Nanotechnology* 13 (2002) 299.
- [6] S. Sze, *Physics of Semiconductor Devices*, 2nd Edition, Wiley, New York, 1981, p. 270.
- [7] M. Macucci, A. Galick, U. Ravaioli, *Phys. Rev. B* 52 (1995) 5210.
- [8] M. Büttiker, *Phys. Rev. Lett.* 65 (1990) 2901.
- [9] A. Kolek, A.W. Stadler, G. Haldaś, *Phys. Rev. B* 64 (2001) 075202.
- [10] M. Macucci, G. Iannaccone, B. Pellegrini, in: *Proceedings of the 15th International Conference on Noise in Physical Systems and $1/f$ Fluctuations*, Hong Kong, August 23–26, 1999, p. 325.
- [11] F. Stern, W.E. Howard, *Phys. Rev.* 163 (1967) 816.
- [12] M. Macucci, G. Iannaccone, G. Basso, B. Pellegrini, Numerical investigation of shot noise suppression in diffusive conductors, *Phys. Rev. B* 67 (2003) 115339.